



Perfluoro-*tert*-butyl-homoserine as a sensitive ^{19}F NMR reporter for peptide-membrane interactions in solution

Benjamin C. Buer,^a Benjamin J. Levin^a and E. Neil G. Marsh^{a,b,*}

Fluorine (^{19}F) NMR is a valuable tool for studying dynamic biological processes. However, increasing the sensitivity of fluorinated reporter molecules is a key to reducing acquisition times and accessing transient biological interactions. Here, we evaluate the utility of a novel amino acid, *L*-O-(perfluoro-*t*-butyl)-homoserine (pFtBSer), that can easily be synthesized and incorporated into peptides and provides greatly enhanced sensitivity over currently used ^{19}F biomolecular NMR probes. Incorporation of pFtBSer into the potent antimicrobial peptide MSI-78 results in a sharp ^{19}F NMR singlet that can be readily detected at concentrations of 5 μM and lower. We demonstrate that pFtBSer incorporation into MSI-78 provides a sensitive tool to study binding through ^{19}F NMR chemical shift and nuclear relaxation changes. These results establish future potential for pFtBSer to be incorporated into various proteins where NMR signal sensitivity is paramount, such as in-cell investigations. Copyright © 2013 European Peptide Society and John Wiley & Sons, Ltd.

Supporting information may be found in the online version of this article.

Keywords: fluorine NMR; antimicrobial peptide; fluorinated protein; MSI-78

Introduction

The unique chemical properties of fluorine make this most abundant biological element extremely useful both to modify the properties of biological molecules and probe their biological function. The favorable NMR properties of the ^{19}F nucleus have made the incorporation of fluorine into both small molecules and biological macromolecules a sensitive tool for studying protein structure, dynamics, and enzyme mechanism [1–19]. Additionally, the general chemical inertness and increased hydrophobicity of fluorinated compounds has been used extensively to create polymers, drugs, and agrochemicals with favorable physicochemical properties [20,21].

Fluorine NMR has several advantages for studying biological systems. The ^{19}F nucleus is present at 100% abundance and possesses 83% of the sensitivity of proton NMR. The fluorine chemical shift is very sensitive to subtle differences in local electronic environment and, because fluorine is essentially absent in biological systems, there is very little interference from background signals. These favorable properties of the ^{19}F nucleus make it a sensitive reporter of changes to the local chemical environment, such as may occur in protein conformational changes or ligand binding, and allow signal to be observed at low micromolar concentrations – conditions that are applicable to many biological studies.

The focus of this study was to develop a fluorinated amino acid-based probe with improved ^{19}F NMR sensitivity that could readily be incorporated into bio-active peptides thereby allowing biological investigations to be conducted at lower peptide concentrations and/or shorter acquisition times. Commonly used fluorinated amino acids in ^{19}F NMR investigations routinely incorporate either only a single fluorine atom [1–3,5,9,12,13,17] or trifluoromethyl group [4,8,14–18,22]. For many of these

fluorinated amino acids, spin coupling between the fluorine nuclei and the neighboring protons result in peak splitting and consequential signal reduction. To increase signal intensity and circumvent the drawbacks associated with spin coupling, we aimed to synthesize a perfluoro-*t*-butyl-containing amino acid that could be incorporated into peptides by well-established solid phase methods.

Here, we report the synthesis of *L*-O-(perfluoro-*t*-butyl)-homoserine (pFtBSer) and its incorporation as a ^{19}F -probe into the antimicrobial peptide (AMP) MSI-78 [23–26]. AMPs are a diverse class of membrane-active peptides that are present in most multicellular organisms and have shown promise for treating antibiotic-resistant bacterial infections [27–31]. These small (12–50 residues) peptides are part of the innate immune system, providing a first line of defense against infection by microorganisms. AMPs function primarily by disrupting the bacterial membrane. Electrostatic interactions between positively

* Correspondence to: E. Neil G. Marsh, Department of Chemistry, University of Michigan, Ann Arbor, MI 48109, USA. E-mail: nmarsh@umich.edu

^a Department of Chemistry, University of Michigan, Ann Arbor, MI 48109, USA

^b Department of Biological Chemistry, University of Michigan Medical School, Ann Arbor, MI 48109, USA

Abbreviations: NMR, nuclear magnetic resonance; AMP, antimicrobial peptide; pFtBSer, *L*-O-(perfluoro-*t*-butyl)-homoserine; tFeG, trifluoroethylglycine; THF, tetrahydrofuran; DIAD, diisopropyl azodicarboxylate; TFA, trifluoroacetic acid; SPPS, solid phase peptide synthesis; HPLC, high performance liquid chromatography; Fmoc, fluorenylmethyloxycarbonyl; MALDI-MS, matrix-assisted laser desorption ionization mass spectrometry; PBS, phosphate buffered saline; CD, circular dichroism; SDS, sodium dodecyl sulfate; MIC, minimal inhibitory concentration; CPMG, Carr–Purcell–Meiboom–Gill.

charged residues in the AMP and the negatively charged lipid head groups that predominate in bacterial membranes initiate AMP binding. Once bound, AMPs may disrupt the lipid bilayer by various mechanisms including the formation of toroidal pores, as is the case for MSI-78. MSI-78 undergoes a conformational change from unstructured to α -helical upon lipid binding. We have previously used MSI-78 labeled with trifluoroethylglycine (tFeG) [4,16] to study this interaction. These earlier studies provide a benchmark by which we can compare the signal intensity and lipid binding induced chemical shift changes of the pFtBSer-containing MSI-78 analogs.

Material and Methods

Synthesis of pFtBSer

(*S*)-2-((*tert*-butoxycarbonyl)amino)-4-hydroxybutanoic acid (**1**)

L-homoserine (5.0 g, 42 mmol) was dissolved in 50 ml THF and 75 ml H₂O then cooled to 0 °C. Sodium bicarbonate (10.58 g, 126 mmol) was added slowly to the stirring mixture followed by addition of di-*t*-butyl dicarbonate (13.75 g, 63 mmol). The reaction was allowed to warm to room temperature, and progress followed via TLC. Upon completion, the mixture was cooled to 0 °C and acidified to pH 2 with 1 M HCl. THF was removed by rotary evaporation, and the resultant mixture was extracted with ethyl acetate (4 × 80 ml). The ethyl acetate layers were combined and washed with sat. aq. NaCl solution (100 ml), dried over Na₂SO₄, filtered and concentrated to give **1** as a clear oil (7.6 g, 84% yield). ¹H NMR (400 MHz, CD₃OD): δ 4.02–3.92 (dd, *J* = 7.2, 4.8 Hz, 1H), 3.61–3.53 (m, 2H), 1.69–2.05 (dm, *J* = 96 Hz, 2H), 1.34 (s, 9H). See Figure S1 for spectrum.

(*S*)-methyl 2-((*tert*-butoxycarbonyl)amino)-4-hydroxybutanoate (**2**)

Generation of diazomethane required the use of appropriate glassware, free of scratches or ground glass. KOH (5.0 g) was dissolved in 8 ml H₂O and 10 ml ethanol in a round bottom flask equipped with a Teflon stir bar. To this, Diazald (5.86 g) dissolved in 75 ml diethyl ether was added. This flask was slowly warmed from room temperature to 50 °C as ethereal diazomethane was directly distilled into the reaction flask containing **1** (2.0 g, 9.18 mmol) dissolved in 25 ml ethyl acetate. After distillation of diazomethane was complete, the reaction flask was gently heated at 40 °C followed by rotary evaporation to concentrate giving **2** as a light yellow solid (2.0 g, 93% yield). ¹H NMR (400 MHz, CD₃OD): δ 4.26–4.20 (dd, *J* = 8.8, 4.4 Hz, 1H), 3.67 (s, 3H), 3.62–3.52 (m, 2H), 2.00–1.72 (dm, *J* = 71.6 Hz, 2H), 1.40 (s, 9H). See Figure S2 for spectrum.

(*S*)-methyl 2-((*tert*-butoxycarbonyl)amino)-4-((1,1,1,3,3,3-hexafluoro-2-(trifluoromethyl)propan-2-yl)oxy)butanoate (**3**)

Ph₃P (3.38 g, 12.87 mmol) was added to **2** (2.0 g, 8.58 mmol) dissolved in 60 ml dry THF and stirring in a three-neck round bottom flask fitted with a condenser. The solution was cooled to 0 °C under N₂, and DIAD (2.6 g, 2.53 ml) was added dropwise over 10 min. After stirring for an additional 10 min, perfluoro-*t*-butanol was added dropwise, and the reaction was heated at 50 °C for 20 h. Upon completion, solvent was removed by rotary evaporation, and mixture was directly purified using silica column chromatography with a gradient of 0% to 10% ethyl acetate in hexanes; fractions were combined and solvent removed using rotary evaporation giving **3** as a waxy solid (1.83 g, 49% yield).

¹H NMR (400 MHz, CD₃OD): δ 4.30–4.23 (dd, *J* = 10.0, 4.4 Hz, 1H), 4.20–4.12 (2H) 3.71 (s, 3H), 2.27–1.90 (dm, *J* = 107.6 Hz, 2H), 1.41 (s, 9H). ¹⁹F NMR (376 MHz, CD₃OD): δ 71.69 (s). See Figure S3 for spectra.

(*S*)-2-amino-4-((1,1,1,3,3,3-hexafluoro-2-(trifluoromethyl)propan-2-yl)oxy)butanoic acid (pFtBSer, **4**)

LiOH (250 mg, 10.5 mmol) was slowly added to **3** (1.83 g, 4.2 mmol) dissolved in 40 ml THF and 20 ml H₂O. The reaction stirred for 12 h at room temperature. Upon completion, the mixture was cooled to 0 °C and acidified to pH 2 with 1 M HCl. THF was removed by rotary evaporation, and the resultant mixture was extracted with ethyl acetate (4 × 25 ml). The ethyl acetate layers were combined and washed with sat. aq. NaCl solution (40 ml), dried over Na₂SO₄, filtered, and concentrated. The concentrate of Boc-L-perfluoro-*t*-butyl-homoserine was dissolved in 20 ml of CH₂Cl₂ and cooled to 0 °C before the addition of 2.8 ml TFA. Reaction proceeded at 0 °C for 4 h, and solvent was removed by rotary evaporation followed by three additions of 10 ml toluene and rotary evaporation to remove toluene and residual TFA. No further purification was needed to give **4** as an off-white solid (1.07 g, 76% yield). ¹H NMR (400 MHz, D₂O): δ 4.23–4.12 (dm, *J* = 7.2 Hz, 2H), 3.76–3.70 (t, *J* = 6.4 Hz, 1H), 2.25–2.04 (dm, *J* = 30.8 Hz, 2H). ¹⁹F NMR (376 MHz, D₂O): δ 70.61 (s). See Figure S4 for the spectra.

Peptide Synthesis

Fmoc-protected SPPS on Rink Amide MBHA resin was used to produce all three peptides as described previously. Resin cleavage with TFA/triisopropylsilane/water (95:2.5:2.5) yielded the desired product with no cleavage of the perfluoro-*t*-butyl group observed. All peptides were purified by reverse phase HPLC using a linear gradient of 95% water, 4.9% acetonitrile and 0.1% TFA for solvent A and 9.9% water, 90% acetonitrile and 0.1% TFA for solvent B, with a flow rate of 10 ml/min on a Waters C18 preparatory column. After lyophilization, peptides were dissolved in water to 20 mg/ml, and all residual TFA was removed by passing this solution through a Stratosphere SPE column (Varian), which was conditioned with 5 ml 50:50 water/MeOH. The column was then rinsed with 4 ml methanol, and ten equivalents of formic acid were added to the peptide solution before lyophilization. ¹⁹F NMR spectra confirmed the complete removal of residual TFA; stock peptide concentrations were determined using ¹⁹F NMR with a known concentration of TFA as an internal reference. Peptide identities were confirmed using MALDI-MS with a matrix of α -cyano-4-hydroxycinnamic acid.

Lipid Preparation

(DMPC), 1,2-dimyristoyl-*sn*-glycero-3-phospho-(1'-*rac*-glycerol) (DMPG) and 1,2-dihexanoyl-*sn*-glycero-3-phosphocholine (DHPC) were purchased from Avanti Polar Lipids (Avanti Polar Lipids Inc., Alabaster, Alabama, USA). Isotropic bicelles were made in PBS buffer, pH 7.4 with 10% D₂O by adding a solution of 3:1 DMPC/DMPG to a solution of DHPC giving *q* = 0.5 resulting in a clear, non-viscous solution.

Circular Dichroism

To examine the secondary structure, we recorded CD spectra of peptides with an Aviv 62DS (Aviv Biomedical Inc., Lakewood, New Jersey, USA) spectropolarimeter at 25 °C. Samples typically contained 50 μ M peptide in buffered solution in either the presence or absence of 50 mM SDS micelles.

MIC Determinations

The peptide MIC against *Escherichia coli* K12 were determined by the microdilution antimicrobial assay procedure, using 96-well plates in replicates of four [32]. A 5 ml overnight culture of *E. coli* was grown in 2xYT media and transferred to 100 ml 2xYT media where it was grown to an OD_{600} of 0.4. Cells were then diluted 1:800 in 2xYT media to an OD_{600} of 0.0005, and 100 μl of the OD_{600} 0.0005 media was added to each well of a sterile 96-well plate. Peptides were dissolved to 400 $\mu\text{g}/\text{ml}$ in PBS buffer, and 100 μl peptide solution was added to the 100 μl of the OD_{600} 0.0005 media in the first well of each row giving a final peptide concentration of 200 $\mu\text{g}/\text{ml}$. 100 μl of the first well was then transferred to the second well, effectively diluting the peptide concentration to 100 $\mu\text{g}/\text{ml}$ repeating this with each subsequent well allowed testing of 10 different peptide concentrations, ranging from 200 to 0.39 $\mu\text{g}/\text{ml}$. Plates were incubated overnight at 37 °C and checked for growth by eye.

^{19}F NMR

All ^{19}F NMR experiments were performed at 30 °C using a Varian (Varian Inc., Palo Alto, California, USA) VNMRS 500 MHz NMR spectrometer equipped with PFG OneNMR room-temperature probe. Peptide and lipid samples were prepared with 10% D_2O in PBS, pH 7.4. All experiments were referenced to trifluoroacetate ion at 0 ppm. ^{19}F CPMG relaxation dispersion experiments were performed for the three peptides in the free state and in the presence of lipid bicelles (200 mM total lipid concentration, $q=0.5$, long chain lipids 3:1 mol/mol DMPC/DMPG and short chain lipid being DHPC) [33,34]. CPMG delays (τ_{CP}) were varied from 0.5 to 10.0 ms with each data point recorded as a series of standard 1-D transverse relaxation rate measurements with T_2 delays of 0.05, 0.1, 0.2, 0.4, 0.8, and 1.6 ms for free peptide and 0.0125, 0.025, 0.05, 0.1, 0.2, and 0.4 ms for bicelle-bound peptide. Data sets were recorded with acquisition time of 1 s in T_1 along with a 10 s pre-scan delay and eight scans for a net acquisition time of 9 min/data point. Data was processed and analyzed in VNMRJ.

Results and Discussion

A limitation for ^{19}F NMR of fluorinated amino acid-based probes with respect to their sensitivity is the number of equivalent fluorine atoms that can be introduced into the structure. The perfluoro-*t*-butyl (pFtB) group introduces nine chemically equivalent fluorine atoms that, because they are not coupled to adjacent protons, result in a sharp singlet. To introduce this reporter group into peptides, we sought a simple, high yielding synthetic

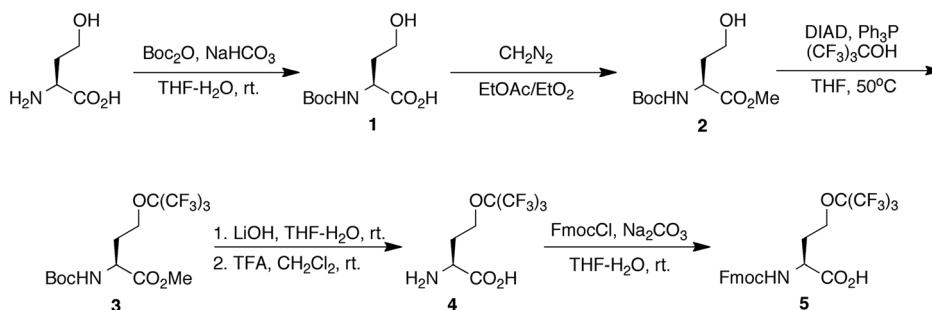
route, the most straightforward approach being to modify an existing natural amino acid. An attractive strategy is to install the pFtB group on an OH-bearing side-chain using a Mitsunobu coupling [35,36] with commercially available perfluoro-*t*-butanol. Our initial attempts to synthesize a pFtB-containing serine analog encountered problems due to β -elimination of perfluoro-*t*-butanol and the formation of anhydroserine as a by-product. We therefore chose to use homoserine as the starting amino acid, which is readily available and relatively inexpensive.

L-O-(perfluoro-*t*-butyl)-homoserine was synthesized straightforwardly from L-homoserine in four steps with an overall yield of 29% (Scheme 1). The synthesis could be accomplished on a multi-gram scale to afford sufficient material for peptide synthesis. Conversion to the Fmoc-protected derivative was accomplished by standard methods and allowed for its incorporation into peptides using standard solid phase peptide synthesis techniques. The perfluoro-*t*-butyl moiety was stable toward both the basic conditions encountered in peptide synthesis and the TFA used to cleave the peptide from the resin. We note that although *t*-butyl ethers can be cleaved by TFA, the perfluoro-*t*-butyl moiety will not support the formation of the intermediate carbocation due to the strongly electron withdrawing nature of the trifluoromethyl groups.

Our previous studies had utilized various analogs of MSI-78 containing the trifluorinated amino acid, tFeG. To directly compare the properties of pFtBSer as a ^{19}F NMR probe with those of tFeG, we synthesized three MSI-78 analogs – MSIF₉-1, MSIF₉-6, and MSIF₉-7, in which pFtBSer is *N*-terminally incorporated or replacing Leu-6 and Lys-7, respectively (Figure 1) and for which analogous tFeG-containing peptides had previously been characterized.

Effect of pFtBSer on the Structure and Activity of MSI-78

As a result of their amphipathic distribution of positively charged and hydrophobic residues, antimicrobial peptides such as MSI-78 undergo a random coil to α -helix transition upon binding lipid bilayers or micelles of anionic detergents such as SDS. As expected, introducing pFtBSer into MSI-78 increased the overall hydrophobicity of the peptide, as determined by analytical HPLC (Figure S5). To evaluate whether the introduction of the more hydrophobic perfluoro-*t*-butyl group interferes with the transition between random coil and α -helix, we recorded the CD spectra of the peptides in buffer and in the presence of SDS micelles. The pFtBSer-containing analogs MSIF₉-1, MSIF₉-6, and MSIF₉-7 each undergo a transition to an extensively α -helical conformation in the presence of SDS micelles as judged by their CD spectra



Scheme 1. Synthetic route of Fmoc-protected L-O-(perfluoro-*t*-butyl)-homoserine (pFtBSer) starting with L-homoserine.

MSI-78 GIGKFLKKAKKFGKAFVKILKK-NH₂
 MSIF₉-1 XGIGKFLKKAKKFGKAFVKILKK-NH₂
 MSIF₉-6 GIGKF^XKKAKKFGKAFVKILKK-NH₂
 MSIF₉-7 GIGKFL^XKAKKFGKAFVKILKK-NH₂

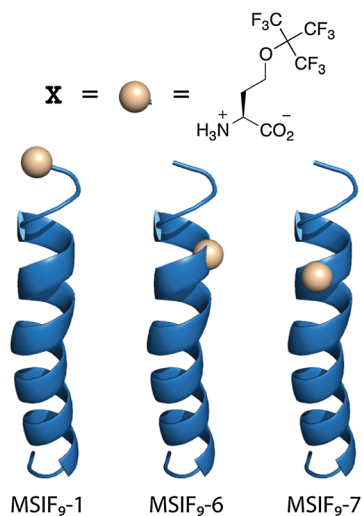


Figure 1. Sequences of the AMP MSI-78 and pFtBSer-containing analogs in this study (top). Cartoon illustrating helical location of pFtBSer in the sequence of MSI-78 analogs (bottom).

(Figure 2). The small differences in helical content between analogs are likely caused by sequence-dependent context effects, which have been noted previously for the incorporation of fluorocarbon amino acids incorporated into α -helical peptides [35].

Having demonstrated that pFtBSer does not impair the ability of MSI-78 to form helical structure, we next investigated whether the pFtBSer-containing analogs would exhibit similar antibacterial activity as the wild-type MSI-78. MSIF₉-1, MSIF₉-6, and MSIF₉-7 peptides each exhibited MIC values of approximately 4 μ g/ml against *E. coli* K12 strains, values that are similar to MSI-78 and previously studied tFeG-containing MSI-78 analogs [4,16,36]. We note that the perfluoro-*t*-butyl group also seems to lower peptide solubility in bacterial medium. MSIF₉-1, MSIF₉-6, and MSIF₉-7 each showed some precipitation at concentrations above 800 μ g/ml

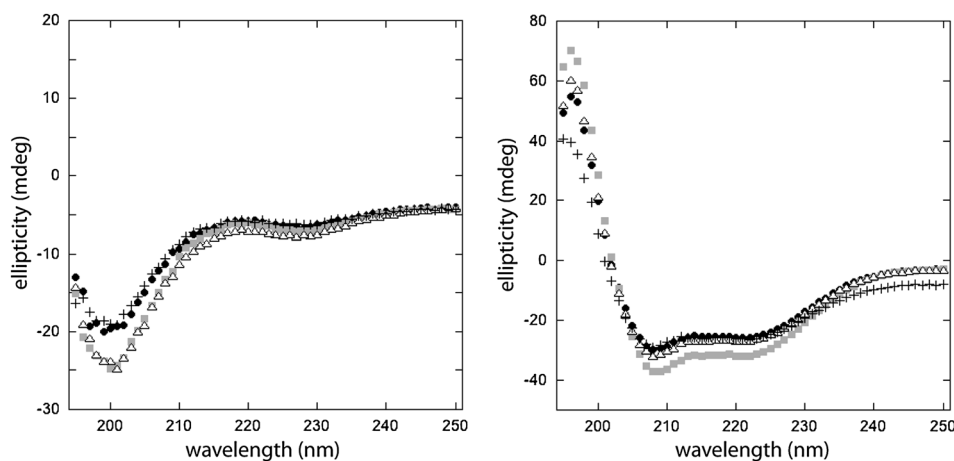


Figure 2. CD spectra of 50 μ M MSI-78 (+), MSIF₉-1 (●), MSIF₉-6 (■), and MSIF₉-7 (Δ) in PBS (left) and in the presence of 50 mM SDS with PBS (right).

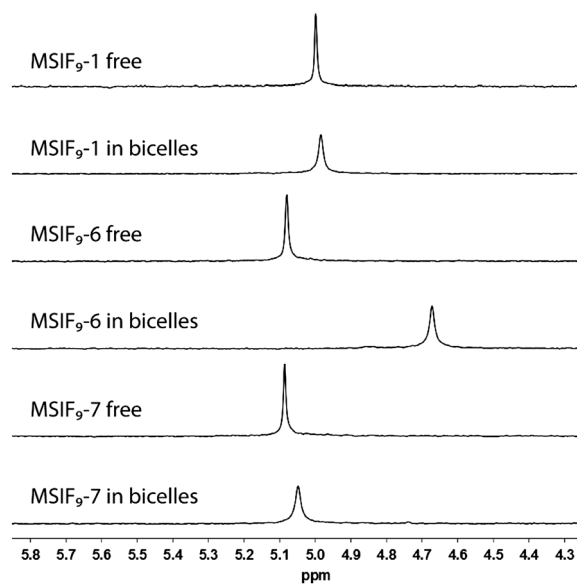


Figure 3. ¹⁹F NMR spectral changes associated with MSIF₉-1, MSIF₉-6, and MSIF₉-7 binding to bicelles. Peptide concentrations in all experiments are 100 μ M; bicelles are at 200 mM total lipid concentration. Spectra were recorded at 30 °C at pH 7.4 in PBS buffer with 10% D₂O and referenced to TFA. All spectra are at 470 MHz with 512 scans and 2 Hz line broadening.

(approximately 300 μ M) in a 50:50 mixture of 2xYT medium and PBS buffer at pH 7.4, although the peptides were soluble at 2 mM as stock solutions in plain PBS. The reason for their reduced solubility in culture media is unclear.

¹⁹F NMR to Probe Lipid Binding of MSIF₉-1, MSIF₉-6, and MSIF₉-7

The retention of native-like structure and antimicrobial activity indicated that pFtBSer-containing MSI-78 analogs would be suitable probes for investigating lipid binding using ¹⁹F NMR. All three pFtBSer-containing peptides display a sharp singlet in the ¹⁹F NMR spectrum between 5.0 and 5.09 ppm relative to trifluoroacetate (internal standard) (Figure 3). Differences in chemical shift between peptides in buffered solution are apparent, demonstrating that the side-chain reporter is sensitive to its position within the sequence. Lipid bicelles were used as a model membrane surface to examine

the interactions of MSIF₉-1, MSIF₉-6, and MSIF₉-7. Introducing pFtBSer at position six results in the greatest change in chemical shift on binding to bicelles, shifting upfield by 0.41 ppm (Figure 3). MSIF₉-7 displays a smaller but still distinct change in chemical shift with an upfield shift of 0.04 ppm upon bicelle binding. MSIF₉-1 has the smallest change in chemical shift upon lipid binding of 0.02 ppm. This pattern of chemical shift changes is qualitatively similar to that previously observed in tFeG-containing MSI-78 analogs (Table 1).

We compared directly the sensitivity of the pFtBSer-containing peptides MSIF₉-1, MSIF₉-6, and MSIF₉-7 with the tFeG-containing peptide MSIF₃-7 for monitoring lipid binding using lipid bicelles. Under the conditions of the experiment (128 scans at 470 MHz, $T=30^\circ\text{C}$), 5 μM concentrations of the pFtBSer-containing peptides were sufficient to observe a signal-to-noise ratio of >4 . In contrast, no ^{19}F signal was discernable for MSIF₃-7 at 5 μM (Figure 4); 50 μM MSIF₃-7 was needed to obtain a ^{19}F signal of similar signal-to-noise ratio.

Although the signal-to-noise ratio is greatly enhanced by using pFtBSer as an NMR reporter, the changes in chemical shift between free and lipid-bound states are smaller than those for tFeG-containing peptides. Thus, the peptides MSIF₃-6 and MSIF₃-7, which incorporate tFeG, displayed changes in chemical shift of 1.30 and 0.22 ppm, respectively upon binding

to bicelles [16], whereas for MSIF₉-6, MSIF₉-7, and MSIF₉-1 the chemical shifts change by 0.41 and 0.04 and 0.02 ppm, respectively. Nevertheless, the chemical shift changes upon binding, although smaller, are readily discernable and allow lipid–peptide interactions to be followed at low micromolar concentrations.

The decreased chemical shift sensitivity is most likely due to the increased distance between the perfluoro-*t*-butyl reporter and the peptide backbone. We consider it unlikely that it is due to a significant change in the affinity of the peptide for the lipid bilayer for several reasons. First, similar lipid affinity is reported for numerous MSI-78 analogs with markedly differing sequences, including the parent peptide, magainin-2, which contains five less Lys residues and one less Leu residue than MSI-78 [37,38]. In this context, the substitution of a single residue in MSI-78 by pFtBSer represents a fairly conservative change. Second, weak binding would result in significant additional line broadening because of chemical exchange spin coupling, which we do not observe. Lastly, MSIF₉-1, MSIF₉-6, and MSIF₉-7 all exhibit similar transitions from unstructured to α -helical in the presence of SDS or lipids and exhibit similar MIC values.

To examine how the mobility of the perfluoro-*t*-butyl side-chain changes when bound to lipid bicelles, we performed a ^{19}F CPMG NMR experiment. The R_2 ($1/T_2$) values, which depend upon local motion of the peptide, were measured for all three

Table 1. Comparison of ^{19}F chemical shifts and R_2 values between MSIF₉ and MSIF₃ peptides

peptide	δ_{free} (ppm)	δ_{bound} (ppm)	$\Delta\delta$ (ppm)	$R_{2\text{free}}$ (Hz)	$R_{2\text{bound}}$ (Hz)
MSIF ₉ -1	5.00	4.98	0.02	1.4 ± 0.1	12 ± 1
MSIF ₉ -6	5.08	4.67	0.41	2.2 ± 0.1	12 ± 1
MSIF ₉ -7	5.09	5.05	0.04	2.1 ± 0.1	15 ± 1
MSIF ₃ -1	12.15	13.34	-1.19	1.7 ± 0.1	27 ± 1
MSIF ₃ -6	11.64	10.34	1.30	3.7 ± 0.1	58 ± 9
MSIF ₃ -7	11.64	11.42	0.22	3.7 ± 0.1	22 ± 2

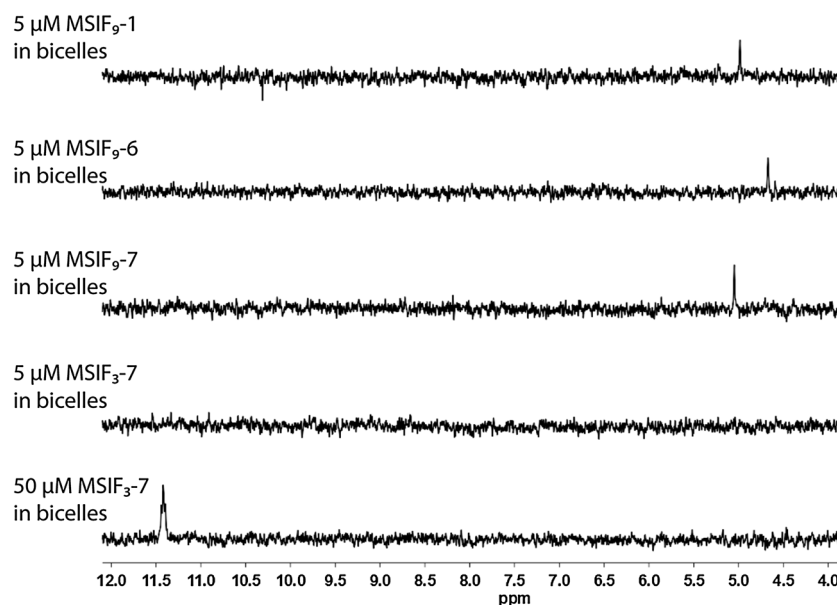


Figure 4. ^{19}F NMR spectral changes associated with low concentrations of MSIF₉-1, MSIF₉-6, MSIF₉-7, and MSIF₃-7 binding to bicelles. Bicelles are at 200 mM total lipid concentration. Spectra were recorded at 30°C at pH 7.4 in PBS buffer with 10% D_2O and referenced to TFA. All spectra are at 470 MHz with 128 scans and 2 Hz line broadening

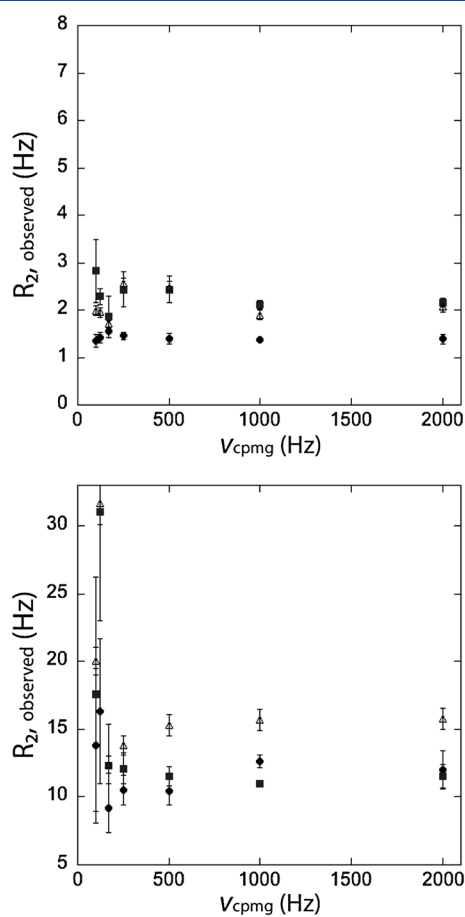


Figure 5. Observed transverse relaxation rate, $R_{2,observed}$, plotted as a function of CPMG pulsing rate (v_{cpmg}). Data are for 100 μ M MSIF₉-1 (●), MSIF₉-6 (■), and MSIF₉-7 (Δ) in buffered solution as unstructured peptides (top) and with 200 mM bicelles (bottom).

MSIF₉ peptides, both in free solution and bound to bicelles, for $1/\tau_{cp}$ ranging from 100 to 2000 Hz (Figure 5). In free solution, all peptides are characterized by R_{2f} of approximately 2 Hz which, as expected, is independent of the CPMG pulsing rate and is consistent with the perfluoro-*t*-butyl group being highly mobile in the unstructured peptide. (For comparison, R_{2f} for the $-CF_3$ group in tFeG-containing MSI-78 variants is approximately 3 Hz) (Table 1) [4,16]. The measurements were then repeated with MSIF₉-1, MSIF₉-6, and MSIF₉-7 bound to high concentrations of lipid bicelles, so that contribution to $R_{2,obs}$ due to free peptide is minimal and thus, $R_{2,obs} = R_{2b}$. For MSIF₉-1, MSIF₉-6, and MSIF₉-7, R_{2b} remains between 10 and 15 Hz, for pulsing rates between 100 and 2000 Hz.

The increase in $R_{2,obs}$ for MSIF₉-1, MSIF₉-6, and MSIF₉-7 in the presence of bicelles is consistent with the peptide binding to the lipid bilayer and reflects a decrease in mobility of the reporter nucleus as expected for the decreased tumbling rate for the peptide–bicelle complex. However, the values of $R_{2,obs}$ are relatively insensitive to the position of the label, in contrast to previous studies using tFeG as the reporter group [16]. The insensitivity of $R_{2,obs}$ to changes in the pulsing rates in the CPMG experiments suggest that the perfluoro-*t*-butyl probe remains quite mobile, even when the peptide becomes structured upon binding to the lipid bilayer. Thus, although pFtBSer exhibits high

intrinsic sensitivity as an NMR reporter, due to nine chemically equivalent fluorine atoms, it appears that it is less well suited than tFeG to report upon the changes in peptide dynamics that accompany peptide binding to the lipid bilayer. This is most likely because for tFeG, the trifluoromethyl group is only one carbon removed from the peptide backbone and therefore more sensitive to peptide backbone motions and conformational changes.

Conclusions

The perfluoro-*t*-butyl-containing amino acid pFtBSer can be readily synthesized in multi-gram quantities and incorporated into proteins by standard SPPS methods, providing an easy-to-incorporate, fluorine chemical moiety for ¹⁹F NMR studies. Incorporation of pFtBSer into three different positions in the AMP MSI-78 displayed little adverse effect to the secondary structure or ability to inhibit *E. coli* growth. The chemical shift of the sharp ¹⁹F NMR singlet arising from pFtBSer, when incorporated into three MSI-78 analogs is sensitive to both the position within the peptide and the environment of the peptide thereby allowing peptide–membrane interactions to be measured at low peptide concentrations. One-dimensional ¹⁹F NMR spectra of MSIF₉-1, MSIF₉-6, or MSIF₉-7 at 5 μ M concentration could easily be obtained in 128 scans taking approximately 3 min per experiment to acquire; importantly, this is the concentration range in which most AMPs are biologically active. The low micromolar NMR sensitivity of pFtBSer-containing peptides should prove useful to probe the interactions of membrane-active peptides with living cells.

References

- 1 Ahmed AH, Loh AP, Jane DE, Oswald RE. Dynamics of the S152 glutamate binding domain of GluR2 measured using ¹⁹F NMR spectroscopy. *J. Biol. Chem.* 2007; **282**: 12773–12784.
- 2 Anderluh G, Razpotnik A, Podlesek Z, Maček P, Separovic F, Norton RS. Interaction of the eukaryotic pore-forming cytolyisin equinatoxin II with model membranes: ¹⁹F NMR studies. *J. Mol. Biol.* 2005; **347**: 27–39.
- 3 Bai P, Luo L, Peng Z. Side chain accessibility and dynamics in the molten globule state of α -lactalbumin: a ¹⁹F-NMR study. *Biochemistry* 2000; **39**: 372–380.
- 4 Buer BC, Chugh J, Al-Hashimi HM, Marsh ENG. Using fluorine nuclear magnetic resonance to probe the interaction of membrane-active peptides with the lipid bilayer. *Biochemistry* 2010; **49**: 5760–5765.
- 5 Buffy JJ, Waring AJ, Hong M. Determination of peptide oligomerization in lipid bilayers using ¹⁹F spin diffusion NMR. *J. Am. Chem. Soc.* 2005; **127**: 4477–4483.
- 6 Danielson MA, Falke JJ. Use of ¹⁹F NMR to probe protein structure and conformational changes. *Annu. Rev. Biophys. Biomol. Struct.* 1996; **25**: 163.
- 7 Gerig J. Fluorine NMR of proteins. *Prog. Nucl. Magn. Res. Spectrosc.* 1994; **26**: 293–370.
- 8 Ieronimo M, Afonin S, Koch K, Berditsch M, Wadhvani P, Ulrich AS. ¹⁹F NMR analysis of the antimicrobial peptide PGLa bound to native cell membranes from bacterial protoplasts and human erythrocytes. *J. Am. Chem. Soc.* 2010; **132**: 8822–8824.
- 9 Kitevski-LeBlanc JL, Evanics F, Prosser RS. Approaches for the measurement of solvent exposure in proteins by ¹⁹F NMR. *J. Biomol. NMR* 2009; **45**: 255–264.
- 10 Kitevski-LeBlanc JL, Prosser RS. Current applications of ¹⁹F NMR to studies of protein structure and dynamics. *Prog. Nucl. Magn. Res. Spectrosc.* 2012; **62**: 1–33.
- 11 Koch K, Afonin S, Ieronimo M, Berditsch M, Ulrich A. Solid-state ¹⁹F-NMR of peptides in native membranes. *Top. Curr. Chem.* 2012; **306**: 89–118.
- 12 Lau E, Gerig J. Origins of fluorine NMR chemical shifts in fluorine-containing proteins. *J. Am. Chem. Soc.* 2000; **122**: 4408–4417.

- 13 Li C, Lutz EA, Slade KM, Ruf RAS, Wang GF, Pielak GJ. ¹⁹F NMR studies of α -synuclein conformation and fibrillation. *Biochemistry* 2009; **48**: 8578–8584.
- 14 Shi P, Wang H, Xi Z, Shi C, Xiong Y, Tian C. Site-specific ¹⁹F NMR chemical shift and side chain relaxation analysis of a membrane protein labeled with an unnatural amino acid. *Protein Sci.* 2011; **20**: 224–228.
- 15 Suzuki Y, Brender JR, Hartman K, Ramamoorthy A, Marsh ENG. Alternative pathways of human islet amyloid polypeptide aggregation distinguished by ¹⁹F NMR-detected kinetics of monomer consumption. *Biochemistry* 2012; **51**: 8154–8162.
- 16 Suzuki Y, Buer BC, Al-Hashimi HM, Marsh ENG. Using fluorine nuclear magnetic resonance to probe changes in the structure and dynamics of membrane-active peptides interacting with lipid bilayers. *Biochemistry* 2011; **50**: 5979–5987.
- 17 Wang GF, Li C, Pielak GJ. ¹⁹F NMR studies of α -synuclein-membrane interactions. *Protein Sci.* 2010; **19**: 1686–1691.
- 18 Maisch D, Wadhvani P, Afonin S, Bottcher C, Koksche B, Ulrich AS. Chemical labeling strategy with (R)- and (S)-trifluoromethylalanine for solid state ¹⁹F NMR analysis of peptaibols in membranes. *J. Am. Chem. Soc.* 2009; **131**: 15596–15597.
- 19 Salwiczek M, Nyakatura EK, Gerling UIM, Ye S, Koksche B. Fluorinated amino acids: compatibility with native protein structures and effects on protein–protein interactions. *Chem. Soc. Rev.* 2012; **41**: 2135–2171.
- 20 Hagmann WK. The many roles for fluorine in medicinal chemistry. *J. Med. Chem.* 2008; **51**: 4359–4369.
- 21 Müller K, Faeh C, Diederich F. Fluorine in pharmaceuticals: looking beyond intuition. *Science* 2007; **317**: 1881–1886.
- 22 Dewel H, Daub E, Robinson V, Honek JF. Incorporation of trifluoromethionine into a phage lysozyme: implications and a new marker for use in protein ¹⁹F NMR. *Biochemistry* 1997; **36**: 3404–3416.
- 23 Fuchs PC, Barry AL, Brown SD. *In vitro* antimicrobial activity of MSI-78, a magainin analog. *Antimicrob. Agents Chemother.* 1998; **42**: 1213–1216.
- 24 Gottler LM, Ramamoorthy A. Structure, membrane orientation, mechanism, and function of pexiganan—a highly potent antimicrobial peptide designed from magainin. *BBA Biomembranes* 2009; **1788**: 1680–1686.
- 25 Hallock KJ, Lee DK, Ramamoorthy A. MSI-78, an analogue of the magainin antimicrobial peptides, disrupts lipid bilayer structure via positive curvature strain. *Biophys. J.* 2003; **84**: 3052–3060.
- 26 Porcelli F, Buck-Koehntop BA, Thennarasu S, Ramamoorthy A, Veglia G. Structures of the dimeric and monomeric variants of magainin antimicrobial peptides (MSI-78 and MSI-594) in micelles and bilayers, determined by NMR spectroscopy. *Biochemistry* 2006; **45**: 5793–5799.
- 27 Brogden KA. Antimicrobial peptides: pore formers or metabolic inhibitors in bacteria? *Nat. Rev. Microbiol.* 2005; **3**: 238–250.
- 28 Huang HW. Action of antimicrobial peptides: two-state model. *Biochemistry* 2000; **39**: 8347–8352.
- 29 Shai Y. Mechanism of the binding, insertion and destabilization of phospholipid bilayer membranes by α -helical antimicrobial and cell non-selective membrane-lytic peptides. *BBA Biomembranes* 1999; **1462**: 55–70.
- 30 Wimley WC. Describing the mechanism of antimicrobial peptide action with the interfacial activity model. *ACS Chem. Biol.* 2010; **5**: 905.
- 31 Wu M, Maier E, Benz R, Hancock REW. Mechanism of interaction of different classes of cationic antimicrobial peptides with planar bilayers and with the cytoplasmic membrane of *Escherichia coli*. *Biochemistry* 1999; **38**: 7235–7242.
- 32 Shelburne CE, An FY, Dholpe V, Ramamoorthy A, Lopatin DE, Lantz MS. The spectrum of antimicrobial activity of the bacteriocin subtilosin A. *J. Antimicrob. Chemother.* 2007; **59**: 297–300. doi: 10.1093/jac/dkl495
- 33 Dubois BW, Evers AS. Fluorine-19 NMR spin-spin relaxation (T₂) method for characterizing volatile anesthetic binding to proteins. analysis of isoflurane binding to serum albumin. *Biochemistry* 1992; **31**: 7069–7076.
- 34 Luz Z, Meiboom S. Nuclear magnetic resonance study of the protolysis of trimethylammonium ion in aqueous solution—order of the reaction with respect to solvent. *J. Chem. Phys.* 1963; **39**: 366.
- 35 Chiu HP, Suzuki Y, Gullickson D, Ahmad R, Kokona B, Fairman R, Cheng RP. Helix propensity of highly fluorinated amino acids. *J. Am. Chem. Soc.* 2006; **128**: 15556–15557.
- 36 Gottler LM, Lee HY, Shelburne CE, Ramamoorthy A, Marsh ENG. Using fluorous amino acids to modulate the biological activity of an antimicrobial peptide. *ChemBiochem* 2008; **9**: 370–373. doi: 10.1002/cbic.200700643|ISSN 1439–4227
- 37 Chen HC, Brown JH, Morell JL, Huang C. Synthetic magainin analogues with improved antimicrobial activity. *FEBS Lett.* 1988; **236**: 462–466.
- 38 Matsuzaki K, Murase O, Tokuda H, Funakoshi S, Fujii N, Miyajima K. Orientational and aggregational states of magainin 2 in phospholipid bilayers. *Biochemistry* 1994; **33**: 3342–3349.